Effect of Hydroxylic Solvent on the Fluorescence Behavior of Some Bioactive 9-Oxo-imidazo[1,2-*a*]purine Derivatives

Grazyna Wenska,*,† Jacek Koput,† Tomasz Pedzinski,† Bronislaw Marciniak,† Jerzy Karolczak,‡ and Bozenna Golankiewicz§

Faculty of Chemistry, A. Mickiewicz University, Grunwaldzka 6, 60-780 Poznan, Poland, Faculty of Physics, A. Mickiewicz University, Umultowska 85, 61-614 Poznan, Poland, Center for Ultrafast Laser Spectroscopy, A. Mickiewicz University, Umultowska 85, 61-614 Poznan, Poland, and Institute of Bioorganic Chemistry, Polish Academy of Sciences, Noskowskiego 12/14, 61-704 Poznan, Poland

Received: May 2, 2006; In Final Form: July 3, 2006

The spectral and photophysical behavior of four fluorescent 9-oxo-imidazo[1,2-*a*]purine derivatives containing pyridyl, pyridylphenyl, phenyl, and biphenylyl substituents at the C(6) position of the tricyclic skeleton is described. The studies were performed in several aprotic and protic organic solvents using absorption spectroscopy as well as steady-state and time-resolved fluorescence spectroscopy. The results are also presented of TDDFT calculations on singlet−singlet excitation energies and oscillator strengths for two models of 9-oxo-imidazo[1,2-*a*]purine, with phenyl or pyridyl substituents, both in the gas phase and in methanol solution. While the derivatives with aryl substituents did not show any significant dependence of their static and dynamic fluorescence properties on the nature of the solvent, the compounds containing a pyridine residue exhibited a remarkable reduction of their fluorescence quantum yields and lifetimes in the alcoholic solutions. The solute−solvent hydrogen-bonding interaction in the first excited singlet state is responsible for the fast radiationless decay rates determined for pyridyl- and pyridylphenyl-substituted compounds in protic solvents. The results of experimental and theoretical studies show that the hydrogen of the alcohols' hydroxyl group and the nitrogen atom of the pyridine moiety are involved in the interaction. The fluorescence-quenching experiments performed for the pyridyl-substituted 9-oxo-imidazo[1,2-*a*]purine derivative using trifluoroethanol, methanol, and butanol as quenchers revealed that the quenching efficiencies, expressed by the Stern−Volmer quenching constants, correlate with the H-bond donating abilities of the alcohols. The quenching is a dynamic process, and the H-bonded complex formed is nonfluorescent. The experimentally determined and the calculated values of the dipole moment change associated with the electronic excitation indicate that the excited S_1 states of all of the molecules studied in this work have an intramolecular charge-transfer character and that electronic charge is transferred to the C(6) substituent upon excitation. Thus, the ability of the pyridyl substituent nitrogen atom to act as an H-bond acceptor in the excited S_1 state is enhanced. The 6-pyridyl-9-oxo-imidazo-[1,2-*a*]purine presents a novel fluorophore, which, besides its medical applications, may be useful as a sensor of hydroxyl groups in microorganized systems.

1. Introduction

3,5-Dihydro-9-oxo-imidazo[1,2-*a*]purine (Chart 1) and other tautomeric forms of the molecule (3,4-dihydro- and 1,4-dihydro-) constitute a basic chromophore of several biologically important molecules.[1−4] In particular, the derivative, carrying the hydroxyethoxymethyl substituent at the N(3) position and the methyl group at the C(6) (Chart 1), exhibits marked antiviral activity similar to the guanine-containing drug, acyclovir (ACV, Chart 1).[1] The tricyclic derivative of ACV, containing a phenyl substituent at the C(6) position (TACV−Ph, Chart 1), exhibits similar antiviral potential but, in contrast to ACV and the C(6)−CH_3-substituted tricyclic derivative, emits fluorescence at room temperature.[5] A combination of these two features is interesting from the point of view of the possible applications of the compound. The intrinsic fluorescence of the bioactive compound could be useful in medical diagnostics[6,7] or employed in the study of mechanisms responsible for the antiviral activity of the acyclovir derivatives.[8] In searching for the most suitable compound for such applications, several derivatives based on the 9-oxo-imidazo[1,2-*a*]purine chromophore have been synthesized.[9−12] The compounds contain various substituted benzene and heterocyclic rings appended at the C-6 position of their tricyclic skeleton. To understand the factors that influence their fluorescence behavior, we have initiated a systematic spectral and photophysical study devoted to this chromophoric system.[13]

In this paper, we focus on the divergent fluorescence properties of the four derivatives containing the 9-oxo-imidazo[1,2-*a*]purine skeleton. The structures of the compounds are presented in Chart 1. The compounds denoted TACV−Py and TACV−Ph−Py contain a pyridine or a phenylpyridine residue, respectively, in the C(6) position of the tricyclic ring, while TACV−Ph and TACV−Ph−Ph are their hydrocarbon analogues. Preliminary fluorescence measurements performed in alcohol and aqueous solutions indicated that the fluorescence behavior of both

* Corresponding author. Tel.: +48-61-829-13-51. Fax: +48-61-865-80-08. E-mail: gwenska@amu.edu.pl.
† Faculty of Chemistry, A. Mickiewicz University.
‡ Faculty of Physics, A. Mickiewicz University and Center of Ultrafast Laser Spectroscopy.
§ Polish Academy of Sciences.

10.1021/jp062680j CCC: $33.50
Published on Web 09/06/2006

CHART 1: Structures of the Compounds

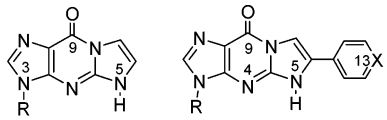

3,5-dihydro-9-oxo-imidazo-[1,2-a]-purine

TACV-Ph X = CH, R = hem
TACV-Ph' X = CH, R = CH_3
TACV-Py X = N, R = hem
TACV-Py' X = N, R = CH_3

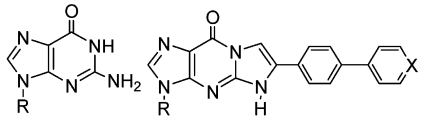

ACV

TACV-Ph-Ph X = CH, R = hem
TACV-Ph-Ph' X = CH, R = CH_3
TACV-Ph-Py X = N, R = hem
TACV-Ph-Py' X = N, R = CH_3

hem = $CH_2OCH_2CH_2OH$

groups of compounds, with and without the pyridyl substituent, differed dramatically. The fluorescence of TACV−Py and TACV−Ph−Py in methanol solution was very weak, and their room temperature emission was barely detectable in aqueous solution ($\phi_F < 10^{-4}$).[10] In general, a variety of factors could be responsible for this dramatically different behavior between these two groups of compounds. These factors include configurations (π,π^* or n,π^*) of the fluorescent states, polar-solvent induced enhancement of nonradiative decay rate, ground- or excited-state specific solute−solvent interactions (H-bonding), or excited-state reactions (phototautomerization). The objective of this work was therefore to reveal the mechanism responsible for the reduced fluorescence yield determined for the pyridyl-substituted compounds in hydroxylic solvents relative to that of the phenyl-substituted ones. The question of why such a small structural change (introduction of an N into the phenyl substituent) influences the photophysics of the resulting molecule was interesting particularly because pyridine-type nitrogens are already present in the imidazo[1,2-*a*]purine skeleton (Chart 1) in all of the compounds studied. In this paper, we present and discuss the results obtained from absorption spectroscopy, steady-state, and time-dependent fluorescence measurements. The investigations were performed in selected protic and aprotic organic solvents of different polarity as well as in solvent mixtures. The selection of solvents was limited due to the insolubility of the compounds in less polar, aprotic solvents. The experimental study was supplemented by TDDFT calculations performed for the molecules TACV−Py′ and TACV−Ph′ (Chart 1), which are models for the molecules studied experimentally.

2. Experimental Section

2.1. Materials. Compounds TACV−Ph,[5] TACV−Ph−Ph,[5] TACV−Py,[10] and TACV−Ph−Py[10] were synthesized as described previously. The compounds were purified by repeated crystallization (at least twice) from CH_3OH. The pure samples were dried over P_2O_5. The purity of the compounds was checked by HPLC (Waters 600 E) equipped with a Waters 991 Photodiode Array absorption detector and a Waters 470 scanning fluorescence detector. The HPLC analyses were carried out on a reversed phase column (X-Terra RP18, 3.5 μm, 4.5 × 150 mm) using a CH_3CN−0.005 M phosphate buffer (pH 7) mixture as an eluent. Methanol (99.97% Scharlau), 1-butanol (99.9% Uvasol), 2,2,2-trifluoroethanol (95% Fluka), acetonitrile (99.9% Backer), and ethyl acetate (99.8%) were dried with molecular sieves 3A.

2.2. Instrumentation. UV absorption and steady-state fluorescence spectra were recorded at room temperature in 1 cm × 1 cm quartz cells using a CaryBio spectrophotometer and an LS 50B Perkin-Elmer spectrofluorimeter, respectively. The emission spectra were corrected for instrumental distortion. The samples were excited within their long-wavelength absorption bands, usually at λ_{max}^A. The absorbance of the samples at their excitation wavelengths was $A \leq 0.2$ ($c \leq 2 \times 10^{-5}$ M). The fluorescence quantum yields were determined using a solution of quinine sulfate in 0.1 N sulfuric acid as a standard ($\phi_F = 0.51$).[14] Fluorescence decays were obtained using a TCSPC method. In the nanosecond range, decays were measured with an IBH Consultants (Glasgow, Scotland) model 5000 fluorescence lifetime spectrometer equipped with a NanoLED-17 type diode ($\lambda_{exc} = 295$ nm, fwhm ≈ 800 ps) as an excitation source. The instrument is capable of measuring lifetimes as short as 400 ps. Reconvolution of fluorescence decay curves was performed using the IBH Consultants Version 4 software. The measurements of fluorescence decays in the picosecond-time range were performed on the previously described TCSPC system.[15] The samples were excited at 280 nm. The picosecond lifetimes were determined as described previously.[16−18] The quality of the fits was judged from the χ^2 values ($\chi^2 \leq 1.2$) and the random distribution of weighted residuals. Ludox solutions were used as the reference for the system response. In TCSPC measurements, the fluorescence intensity was monitored at λ_{max}^F unless otherwise stated. Solvents were checked under the conditions used in the fluorescence decay measurements, and they were found to exhibit emission small enough to be disregarded relative to their influence on the lifetimes measured.

2.3. Theoretical Calculation. The equilibrium structural parameters and energetics of the isolated molecules and their hydrogen-bonded complexes were determined using the density functional theory (DFT) approach, the PBE0 model[19] in conjunction with the one-particle basis set of triple-ζ quality 6-311+G-(2df,2pd).[20] To investigate the macroscopic solvent effects, the DFT calculations were also performed using the conductor polarizable continuum model (CPCM).[21] The electronic excited-state energies and transition oscillator strengths were determined using the time-dependent DFT method (TDDFT). The stability of the computed spectra was checked against changes in the basis set or in the number of computed roots. The results were found to be weakly dependent on the basis set. For the first excited-state S_1, which is of main interest here, the PBE0 method in conjunction with the double-ζ basis set 6-31G(d,p) tends to increase the excitation energies by less than ∼0.1 eV (800 cm^{-1}) for all of the species under consideration. Therefore, none of the qualitative conclusions of this work depend on the one-particle basis set used for the DFT calculations. The Gaussian 03 package[22] was employed for all of these calculations.

3. Results and Discussion

3.1. Spectroscopy and Photophysics in Pure Solvents. Absorption spectra of TACV−Py, TACV−Ph−Py, and the respective phenyl-containing congeners, TACV−Ph and TACV−Ph−Ph, in methanol are presented in Figure 1. In the spectral region 230−400 nm, all of the compounds exhibited two intense absorption bands. Introduction of a nitrogen atom into the phenyl substituent does not significantly change the shape of the bands, but it causes a small red shift of the long-wavelength maximum and a small decrease in its intensity. As compared to TACV−Py and TACV−Ph, the presence of an additional phenyl ring in TACV−Ph−Py and TACV−Ph−Ph causes a significant increase in the intensity of both bands, but the positions of the

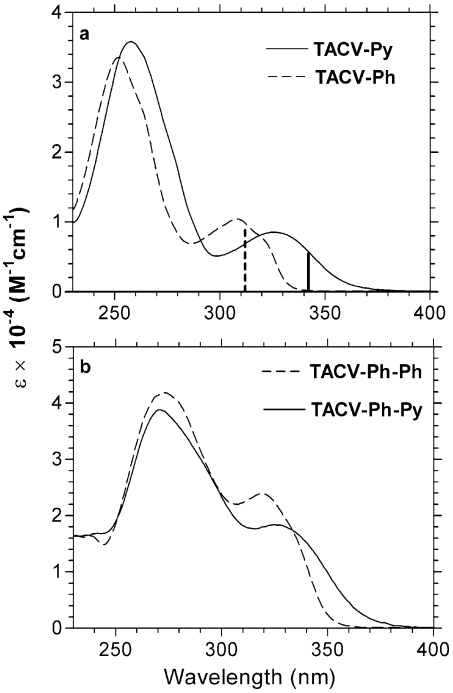

Figure 1. UV−vis absorption spectra in CH_3OH: (a) of TACV−Py and TACV−Ph, (b) of TACV−Ph−Py and TACV−Ph−Ph; vertical lines indicate the predicted (TDDFT) energies of the $S_0 \rightarrow S_1$ transitions for TACV−Py′ (solid line) and TACV−Ph′ (dotted line).

absorption maxima do not shift significantly. The substituent effects indicate that the redistribution of electronic charge upon excitation of the molecules is not confined to the tricyclic imidazopurine system but that it extends onto the C(6) aryl/heteroaryl substituent. The location of the long-wavelength absorption maximum showed a small dependence on solvent properties (Table 1). The small solvent effects, together with high intensity of the lowest-energy absorption band ($\epsilon \geq 10^4$ M^{-1} cm^{-1}), imply that the electronic excitation is of a $\pi \rightarrow \pi^*$ electronic nature. The absorption spectral data for the compounds studied are presented in Table 1.

The fluorescence spectra of the compounds studied in this work were each characterized by a single, structureless band in the 350−650 nm spectral region in all of the solvents used. In parallel with the UV absorption spectra, the fluorescence maxima of the compounds containing the pyridyl and pyridylphenyl substituents were located, in each solvent, at longer wavelengths than their aryl analogues. Parameters characterizing fluorescence spectral properties as well as fluorescence quantum yields and lifetimes are compiled in Table 1.

The effect of solvent polarity on the location of the fluorescence maxima was more pronounced than that on the absorption spectral maxima, and the λ_{max}^F shifts to longer wavelengths in more polar solvents. Thus, the Stokes shift increased with solvent polarity, indicating that the molecules are more polar in their excited states than in their ground states. Application of the Lippert−Mataga relation[23−25] (eq 1) to the Stokes shift values for TACV−Py and TACV−Ph in nonprotic solvents gives straight lines (Figure 2).

$$\nu_A - \nu_F = [2(\Delta\mu)^2/h \times c \times a^3]\, f(D,n) \qquad (1)$$

where $f(D,n) = [(D-1)/(2D+1)] - [(n^2-1)/(2n^2+1)]$, D and n are, respectively, the relative permittivity (dielectric constant) and refractive index of the solvents, ν_A and ν_F are wavenumbers (cm^{-1}) of absorption and fluorescence maxima, respectively, $\Delta\mu = \mu_e - \mu_g$ is the change in dipole moment of the molecules in their excited (μ_e) and in their ground states (μ_g), h is Planck's constant, c is light velocity, and a is the radius of the cavity occupied by the fluorophore molecules.

The slopes of both linear plots presented in Figure 2 are very similar, indicating that the dipole moment changes upon excitation of both molecules into their S_1 states are very similar. The change in the dipole moment following excitation calculated from the slopes of the solvatochromic plots was found to be $\Delta\mu = 11.6$ D for TACV−Py and $\Delta\mu = 11.4$ D for TACV−Ph. The slope of the linear fit to the TACV−Ph data (Figure 2) strongly depends on the value of the Stokes shift measured in $CHCl_3$. When this point was omitted from the least-squares fitting, the value $\mu = 7.3$ D was obtained from the slope (8000 cm^{-1}) of the resulting straight line. In the calculations, the value of solute radius $a \approx 0.5$ nm derived from molecular volumes[22] of TACV−Py′ and TACV−Ph′ was used. The ground and excited-state dipole moments were also computed at the PBE0/6-311+G(2df,2pd) level of theory for the model compounds TACV−Py′ and TACV−Ph′ (see Chart 1). The calculations yield $\mu_g = 6.3$ D and $\mu_e = 21.5$ D for TACV−Py′, and $\mu_g = 7.4$ D and $\mu_e = 17.4$ D for TACV−Ph′. The values of $\Delta\mu$ determined from experimental data and calculations show reasonable agreement. These results clearly indicate that excitation to the S_1 state is associated with significant displacements of electronic charge. The excited S_1 state of both types of molecules, with and without pyridine residues, has clearly an intramolecular charge-transfer character (ICT) (see Figure 7 and discussion below). It should be pointed out that the $\Delta\mu$ values obtained from experiment are only approximate. The Lippert−Mataga relation was derived under certain assumptions such as the molecules being spherical in shape and the ground and excited-state dipole moments being collinear.[23] Neither of these assumptions was fulfilled in the molecular systems studied in this work. The shapes of molecules under consideration are rodlike, and the calculations indicate that the dipole-moment vectors in the ground S_0 state point along the short axis, while in the excited S_1 state the dipole-moment vectors point along the long axis of the molecule.

Fluorescence quantum yields of the compounds, irrespective of the nature of the substituents at the C(6) position, were quite high in the aprotic, less polar solvent EtOAc, particularly in the cases of TACV−Ph−Ph and TACV−Ph−Py. The values of ϕ_F decrease by a factor < 4 in the more polar CH_3CN. In alcohols, ϕ_F values for the compounds TACV−Py and TACV−Ph−Py differ significantly from those of their hydrocarbon analogues TACV−Ph and TACV−Ph−Ph. The fluorescence quantum yields of the pyridyl-substituted compounds decreased by 2 orders of magnitude in CH_3OH as compared to their corresponding values in CH_3CN (Table 1), while the ϕ_F values of TACV−Ph and TACV−Ph−Ph were similar in both solvents. Methanol ($D = 32.66$,[26] $\pi^* = 0.60$[27]) and acetonitrile ($D = 35.94$,[26] $\pi^* = 0.75$[27]) are of comparable polarity expressed by relative permittivity (dielectric constant, D) or π^* scale, but only CH_3OH participates in the formation of hydrogen bonds acting usually as an H donor ($\alpha = 0.63$[27]). Reduction in the ϕ_F values of TACV−Py and TACV−Ph−Py may therefore be related to a specific solute−solvent interaction (hydrogen bonding) rather than to solvent polarity. The reduced fluorescence quantum yields in alcohols due to the specific interactions in the ground or excited state have been observed in several molecular systems: anthraquinone,[28] aminoanthraquinone,[29,30] aminofluorenone derivatives,[31,32] 1-hydroxy-9-fluorenone,[33] 2-amino-7-

TABLE 1: Absorption and Fluorescence Maxima, Fluorescence Quantum Yields, Lifetimes, Radiative, and Nonradiative Rate Constants for Compounds TACV−Py, TACV−Ph, TACV−Ph−Py, and TACV−Ph−Py in Selected Solvents

compound	solvent	λ_{max}^{A} [nm]	λ_{max}^{F} [nm]	ϕ_F	τ [ns]	k_F [10^7 cm^{-1}]	k_{NR} [10^9 cm^{-1}]
TACV−Py	EtOAc	325	425	0.18	9.7	1.9	0.09
	CH_3CN	324	460	0.08	6.2	1.3	0.15
	CH_3OH	326	435	0.001	0.084[a]	1.2	11.9
	C_4H_9OH	326	435	0.006	0.4[a]	1.5	2.5
TACV−Ph	EtOAc	310	385	0.25	4.4	5.7	0.17
	CH_3CN[b]	309	395	0.17	6.2	2.7	0.13
	CH_3OH[b]	308	390	0.14	3.8	3.7	0.23
	C_4H_9OH[b]	310	368	0.17	3.2	5.3	0.26
TACV−Ph−Py	EtOAc	332[c]	445[c]	0.40[c]	6.8	5.9	0.09
	CH_3CN	325[c]	482[c]	0.10[c]	3.2[c]	3.1	0.28
	CH_3OH	327[c]	480[c]	0.002	0.040[a]	5.0	25.0
	C_4H_9OH	325	470	0.04	0.9[a]	4.4	10.7
TACV−Ph−Ph	EtOAc	325	400	0.51	4.3	11.9	0.11
	CH_3CN	319	423	0.36	6.3	5.7	0.10
	CH_3OH	319	405	0.48	4.8	10.0	0.11
	C_4H_9OH	320	395	0.34	3.8	8.9	0.17

[a] Longer-lived component of the biexponential fluorescence decay measured in CH_3OH at $\lambda^F = 460$ nm, in C_4H_9OH at λ^F_{max}; see text. [b] From ref 13. [c] From ref 10.

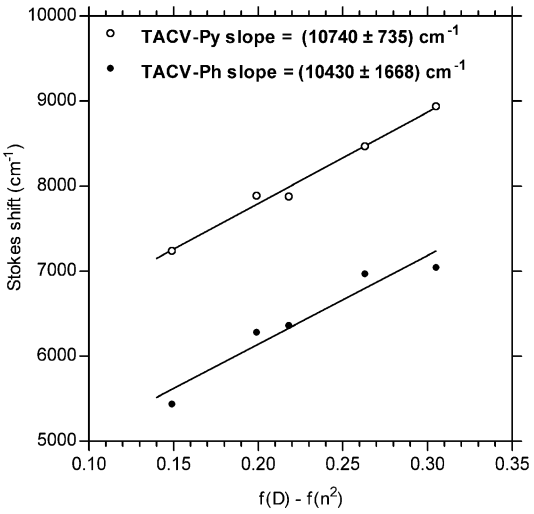

Figure 2. Solvatochromic plots for TACV−Py and TACV−Ph and least-squares fits.

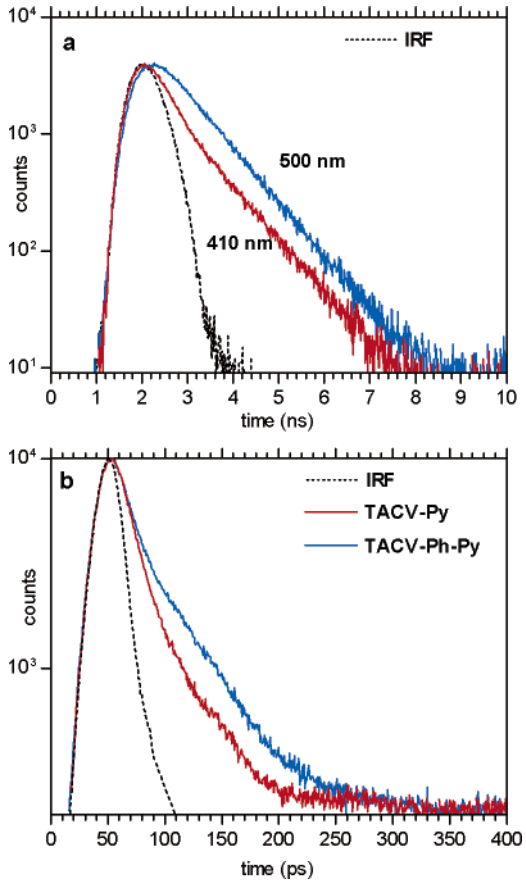

Figure 3. The instrumental response function (IRF) and the experimental fluorescence decay traces: (a) of TACV−Ph−Py in C_4H_9OH at the blue ($\lambda^F = 410$ nm, fit: $\tau_1 = 0.9$ ns, $f_1 = 0.45$; $\tau_2 < 0.1$ ns, $f_2 = 0.55$) and the red edge of the fluorescence band ($\lambda^F = 500$ nm, fit: $\tau_1 = 0.9$ ns, $f_1 = 0.86$; $\tau_2 < 0.1$ ns, $f_2 = 0.14$), $\lambda_{exc} = 295$ nm; (b) of TACV−Py and TACV−Ph−Py in CH_3OH at $\lambda^F = 460$ nm (TACV−Py fit: $\tau_1 = 84$ ps, $f_1 = 0.94$; $\tau_2 = 14$ ps, $f_2 = 0.06$; and TACV−Ph−Py fit: $\tau_1 = 40$ ps, $f_1 = 0.51$; $\tau_2 = 12$ ps, $f_2 = 0.49$), $\lambda_{exc} = 280$ nm, at room temperature.

nitrofluorene,[34] 4-aminophthalimide derivatives,[35] and 2-(2′-pyridyl)indoles.[36−38]

The experimental fluorescence decays measured at the λ_{max}^F of each compound in aprotic solvents could be satisfactorily fitted by monoexponential functions. Moreover, the decays in CH_3CN were confirmed to be single-exponential irrespective of the detection wavelength (at λ_{max}^F and at the blue and red edges of the fluorescence bands). The lifetimes determined from the fitting procedure are listed in Table 1. In alcohols, monoexponential decays were observed exclusively in the case of the aryl-substituted compounds: TACV−Ph and TACV−Ph−Ph. The fluorescence decays of pyridyl- and pyridylphenyl-substituted compounds were fitted to the sum of two exponentials. As an example, the experimental decays of TACV−Ph−Py in C_4H_9OH and TACV−Py and TACV−Ph−Py in CH_3OH are presented in Figure 3. In CH_3OH solutions, the decay lifetimes of both components were shorter than the time resolution of our nanosecond instrument, and, therefore, the kinetics of the fluorescence decays in this solvent were measured by picosecond fluorescence spectroscopy. The lifetimes of the longer-lived species in CH_3OH were determined to be $\tau_1 = 84$ ps for TACV−Py and $\tau_1 = 40$ ps for TACV−Ph−Py. The lifetimes of the short-lived components of both compounds were similar, $\tau_2 = 14$ ps and $\tau_2 = 12$ ps for TACV−Py and TACV−Ph, respectively. In C_4H_9OH the lifetimes of the short-lived components were in the picosecond range ($\tau_2 \leq 0.1$ ns); the lifetimes for the longer-lived component were $\tau_1 = 0.4$ ns and $\tau_1 = 0.9$ ns, for TACV−Py and TACV−Ph, respectively. In the biexponential decays the longer-lived component was dominant at λ_{max}^F (fractional coefficient $f > 0.5$), but the contributions of short-lived component increased on the blue

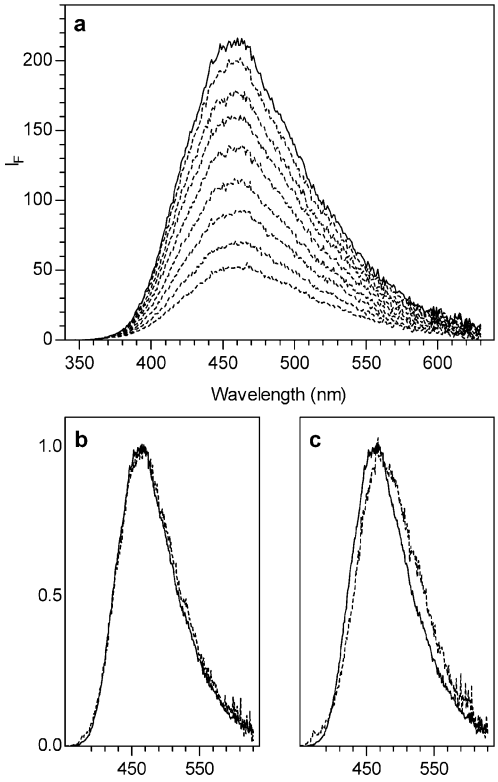

Figure 4. (a) Fluorescence of TACV−Py in CH_3CN without and in the presence of 0.003, 008, 0.014, 0.024, 0.040, 0.060, 0.095, 0.14 M TFE; (b) normalized fluorescence spectra of TACV−Py without (solid line) and in the presence of 0.14 M TFE (dotted line); (c) normalized fluorescence spectra of TACV−Py without (solid line) and in the presence of 0.5 M CH_3OH (dotted line); $\lambda_{exc} = 320$ nm.

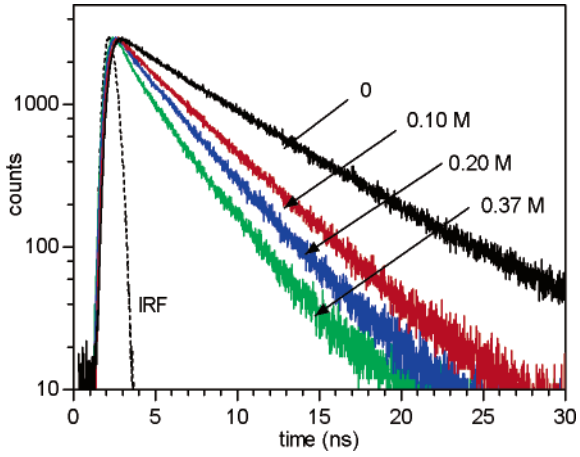

Figure 5. Experimental fluorescence decays of TACV−Py in CH_3CN without (0) and in the presence of CH_3OH at the concentrations 0.10, 0.20, and 0.37 M and the instrumental response function (dotted line); $\lambda_{exc} = 295$ nm, $\lambda^F = 460$ nm.

edge of the band (Figure 3a). The longer-lived components of the decays were identified as the relaxed excited S_1 states of TACV−Py and TACV−Ph−Py in the alcohol solvents, and their values are listed in Table 1.

The presence of species with picosecond lifetimes in the fluorescence decays of TACV−Py and TACV−Ph−Py in alcohol solutions may be related to specific relaxations of solvent around the S_1 excited fluorophore molecules. This kind of fluorescence decay kinetics was previously observed for several molecular systems, in which the excited S_1 states have ICT character. When these molecules are in their excited states, the alcohol molecules form intermolecular H bonds at the acceptor sites of solute molecules.[39−41] The specific solvation time of the S_1 excited state of the aminofluorenone molecules by CH_3OH was reported to be $\tau = 10$ ps.[39] The presence of two fluorescent species in alcoholic solutions of TACV−Py and TACV−Ph−Py cannot be due to the presence of two species in their S_0 states because the shapes of both fluorescence spectra and excitation spectra were found to be independent of wavelength.

The radiative and nonradiative rate constants calculated from experimental data using the relations $k_F = \phi_F/\tau$ and $k_{NR} = (1 - \phi_F)/\tau$ are included in Table 1. A comparison of the k_{NR} values in all solvents indicates that the very low fluorescence quantum yields of TACV−Py and TACV−Ph−Py in alcohols were due to the radiationless processes being 30−100 times faster in these solvents. This specific effect of alcohols on the value of k_{NR} is indicative of an intermolecular H-bonding interaction in the S_1 state as being mainly responsible for the enhanced radiationless deactivation of the excited states of TACV−Py and TACV−Ph−Py molecules. The large value of k_{NR} determined for these molecules is not related to the energy gap law[42] because the S_1–S_0 energy difference (ΔE_{S1-S0}) expressed by $(\nu_A + \nu_F)/2$ in CH_3OH solutions is not smaller than that in CH_3CN (for TACV−Py, $\Delta E_{S1-S0} = 26.8 \times 10^3$ cm^{-1} in CH_3OH and $\Delta E_{S0-S1} = 26.3 \times 10^3$ cm^{-1} in CH_3CN; for TACV−Ph−Py, $\Delta E_{S0-S1} = 25.7 \times 10^3$ cm^{-1} in CH_3OH and in CH_3CN).

In contrast, alcohols do not influence the dynamics of the excited S_1 state decays in the cases of TACV−Ph and TACV−Ph−Ph. The value of k_{NR} for TACV−Ph in the protic solvent (CH_3OH) was only 1.8 times higher than in CH_3CN, and it was almost identical in both solvents in the case of TACV−Ph−Ph. Thus, the crucial role of the nitrogen of the pyridyl substituent (N(13) in TACV−Py, see Chart 1) in the H-bonding interactions can be suggested on the basis of a simple consideration of the structure−fluorescence relationship within the series of the four compounds studied in this work.

3.2. Quenching of TACV−Py Fluorescence by Alcohols. To obtain information on the nature of the specific interactions of pyridyl-containing compounds with alcohols, we carried out a quenching study. Fluorescence of TACV−Py in CH_3CN in the presence of added alcohols 2,2,2-trifluoroethanol (TFE), CH_3OH, and C_4H_9OH was studied by steady-state and time-resolved nanosecond spectroscopy. The alcohols chosen as quenchers differ in their hydrogen-bond donating (α) and hydrogen-bond accepting abilities (β), characterized by the parameters α and β defined by M. J. Kamlet et al.[27] Acetonitrile was the solvent of choice in this study because of the insolubility of the compound in nonpolar aprotic solvents (alkanes). In general, addition of alcohols to the solution of TACV−Py resulted in a reduction of the fluorescence intensity. The spectral changes observed upon addition of TFE are presented in Figure 4. Methanol and butanol were less effective quenchers because higher concentrations of the alcohols were required to attain I_F^0/I_F ratios comparable to those caused by TFE. Moreover, in the cases of CH_3OH and C_4H_9OH, reduction in fluorescence intensities was accompanied by a small red shift of the fluorescence band maxima. The normalized fluorescence spectrum of TACV−Py in the presence of 0.5 M CH_3OH was shifted by ~5 nm, and the shift was less pronounced in the case of C_4H_9OH (~3 nm).

The decay of the TACV−Py fluorescence in the presence of TFE ([TFE] ≤ 0.5 M) was monoexponential irrespective of the monitored wavelength. The lifetimes determined from experimental decay curves were shorter than in pure CH_3CN, and their values gradually decreased with increasing concentrations of

TABLE 2: Lifetimes[a] and Fractional Coefficients[b] Determined from the Decays of TACV−Py in CH_3CN Solution in the Presence of Alcohols Measured with Nanosecond Fluorescence Spectroscopy[c]

λ^F [nm]	CH_3OH (M)	τ_i [ns] (f_i)	C_4H_9OH [M]	τ_i [ns] (f_i)
460	0.10	4.0 (0.96)/0.5 (0.04)	0.06	5.2 (0.95)/0.4 (0.05)
460	0.14	3.6 (0.97)/0.6 (0.03)	0.17	4.0 (0.95)/0.6 (0.05)
460	0.20	3.3 (0.93)/0.6 (0.07)	0.29	3.4 (0.94)/0.6 (0.05)
460	0.28	3.0 (0.95)/0.5 (0.05)	0.48	3.0 (0.93)/0.5 (0.07)
460	0.37	2.8 (0.84)/0.6 (0.16)	0.85	2.6 (0.91)/0.4 (0.09)
460	0.50	1.9 (0.93)/0.2 (0.07)		
450	0.82	1.32 (0.94)/0.18 (0.06)		
450[d]	0.82	1.21 (0.83)/2.55 (0.12)/0.15 (0.05)		
430[d]	0.82	1.20 (0.79)/2.28 (0.11)/0.13 (0.09)		
480[d]	0.82	1.17 (0.74)/3.08 (0.26)		

[a] τ_i. [b] f_i. [c] $\lambda_{exc} = 295$ nm. [d] Measured with picosecond fluorescence spectroscopy, $\lambda_{exc} = 270$ nm.

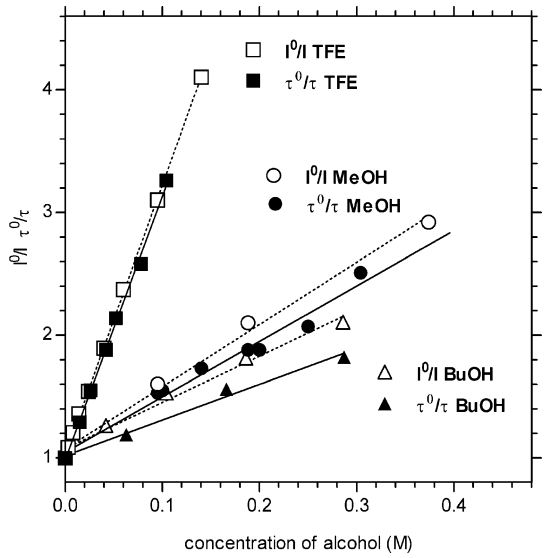

Figure 6. S−V plots for quenching of TACV−Py fluorescence by alcohols in CH_3CN solution.

TFE. The single emitting species was ascribed to the excited S_1 state of the free uncomplexed form of TACV−Py in CH_3CN. The shortening of the lifetime proved that the fluorescence was quenched in a dynamic process. The kinetics of the TACV−Py fluorescence decays in the presence of CH_3OH and C_4H_9OH were more complex. Several experimental traces measured at λ_{max}^F, when CH_3OH was used as the quencher, are presented as examples in Figure 5. The decay of the fluorescence measured at λ_{max}^F could be described by a sum of two exponentials. The results of fitting to the experimental data obtained by nanosecond spectroscopy, when CH_3OH and C_4H_9OH were used as quenchers, are presented in Table 2. The lifetime τ_1 of the species, which mainly contributes ($f_1 > 0.9$) to the fluorescence intensity at λ_{max}^F, is in the nanosecond region. Its lifetime decreased with increasing alcohol concentrations. This species was, therefore, identified as the excited S_1 state of the non-H-bonded form of TACV−Py. The lifetimes of the minor components ($f_2 \leq 0.05$) of the TACV−Py fluorescence decays in the presence of CH_3OH and C_4H_9OH were shorter ($\tau_2 \approx 0.5$ ns). The kinetics of TACV−Py fluorescence quenching by 0.82 M CH_3OH was also studied at three different emission wavelengths with picosecond spectroscopy. The analysis of the decays revealed the presence of three species with lifetimes presented in Table 2. The contributions of the emissions from the three species to the total measured intensity depended on the wavelengths, but, at any of the monitored λ^F, the contribution from the emission with the lifetime $\tau_1 = 1.19 \pm 0.02$ ns was dominant ($f_1 > 0.74$). The emission of the species with the lifetime $\tau_2 = 2.64 \pm 0.44$ ns was red shifted as compared to the fluorescence of the non-H-bonded form of TACV−Py in CH_3CN ($\lambda^F = 430$ nm, $f_2 = 0.11$; $\lambda^F = 480$ nm, $f_2 = 0.26$). It appears that this species could not be ascribed to the H-bonded complex of TACV−Py and CH_3OH because its lifetime was significantly (~30×) longer than that observed in a solvent of similar polarity ($\tau = 0.084$ ns in CH_3OH, Table 1).

Apparently, the difference in quenching behavior of TFE and the remaining alcohols could be related to the possibility of the latter alcohols to act as H-bond acceptors. In such cases, the N(5)H of the TACV−Py molecule (Chart 1) and the oxygen from the alcohols would be involved in the H-bonding interactions. This type of interaction was certainly not responsible for the fluorescence quenching of pyridyl-containing TACV derivatives discussed in this work, and the dynamic quenching, observed in CH_3OH and C_4H_9OH, reflects only the interaction of solute molecules with alcohols acting as H-bond donors. We observed in preliminary experiments that the addition of dimethyl sulfoxide ([DMSO] = 0.8 M) did not change the fluorescence quantum yield ($\lambda_{exc} = 320$ nm) within experimental error although the best fit to the experimental decay curve ($\lambda_{exc} = 295$ nm, $\lambda^F = 460$ nm) was obtained assuming a small contribution ($f_2 \approx 0.04$) from a second component with a lifetime $\tau_2 \approx 1.8$ ns in addition to the lifetime of TACV−Py in pure CH_3CN. Dimethyl sulfoxide can act solely as an H-bond acceptor ($\beta = 0.76$).[20] Finally, nonexponential fluorescence decays in the presence of CH_3OH and C_4H_9OH may reflect the intervention of ground-state H-bonded complexes of TACV−Py. As pointed out earlier, the concentrations of the alcohols used in quenching studies were higher (~4×) than that of TFE. Absorption spectroscopy revealed that addition of any of the alcohols up to a concentration of $c \leq 0.5$ M to the solution of TACV−Py in CH_3CN did not cause changes in the shape and intensity of the long-wavelength absorption band. At higher concentrations of the alcohols ($c > 1.5$ M), a subtle intensity change was observed. Thus, in the S_0 state, the fraction of TACV−Py molecules intermolecularly bonded to alcohol molecules is small and/or the H-bonded forms are not distinguishable by UV absorption spectroscopy. H-bonded forms could include bonding at various positions in TACV−Py, that is, N(1), C═O, N(4), and N(13) (see Chart 1 for atom numbering). Indeed, the computational results showed that the UV spectra of the various H-bonded complexes of the TACV−Py′ molecule did not differ significantly from those of the free, uncomplexed TACV−Py′ molecule (vide infra). Because static quenching had only very minor contributions to the total measured fluorescence quenching of TACV−Py (vide infra) and because of the complexity of the system (TACV−Py molecule has several sites that may interact with alcohol molecules), we did not attempt further to identify the minor emitting species observed in time-resolved quenching studies.

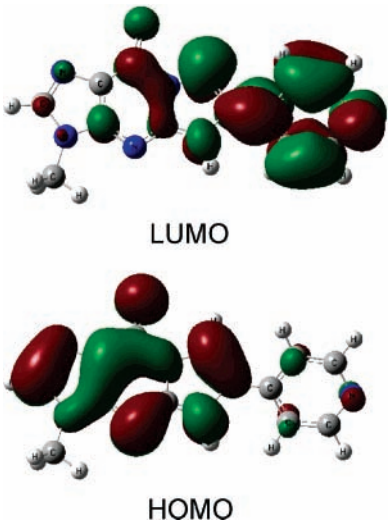

Figure 7. The shapes of the HOMO and LUMO involved in the $S_0 \rightarrow S_1$ transition of TACV−Py computed at the PBE0/6-311+G(2df,2pd) level of theory.

TABLE 3: Stern−Volmer Constants[a,b] and Rate Constants[c] for Quenching of TACV−Py Fluorescence by Alcohols[d]

alcohol	TFE	CH_3OH	C_4H_9OH
α[e]	1.51	0.62	0.79
β[e]	0.00	0.93	0.88
K_{SV}'[a]	22.0 ± 0.1	5.1 ± 0.2	3.8 ± 0.3
K_{SV}[b]	21.4 ± 0.5	4.5 ± 0.1	2.9 ± 0.2
$k_Q \times 10^{-9}$ [c]	4.0	0.8	0.5

[a] Stern−Volmer constant [M^{-1}] from measurements of the intensities at λ_{max}^F. [b] Stern−Volmer constant [M^{-1}] from lifetime measurements. [c] Quenching rate constant [M^{-1} s^{-1}] calculated from lifetime data. [d] In CH_3CN solution. [e] From ref 27.

To compare the quenching efficiency of the various alcohols, we used the Stern−Volmer relation,[23] and the resulting linear plots are presented in Figure 6. In the case of TFE, the Stern−Volmer constant K_{SV}' derived from the slope of the plot I_F^0/I_F versus alcohol concentration was, within experimental error, the same as the K_{SV} calculated from the τ^0/τ versus [alcohol] plot (Table 3). When CH_3OH and C_4H_9OH were used as quenchers, the slopes of the plots constructed from the measurement of the area under the entire fluorescence bands (ϕ^0/ϕ) were only slightly (<10%) higher than that constructed from intensities at the λ_{max}^F. This indicated that the contribution of emission from the noncomplexed form of TACV−Py to the total emission spectrum was predominant and that the quantum yield of any red shifted emission was low. When lifetimes, attributed to the S_1 excited state of free TACV−Py, were used to construct S−V plots, the slopes of the resulting lines were not much different from the slopes of the S−V plots from static measurements (Figure 6 and Table 3). This indicates that there could only be a small contribution from static quenching. The efficiency of quenching determined by K_{SV} showed good correlation with the parameter α characterizing the hydrogen-bond donating ability of alcohols. For example, TFE, which has the highest hydrogen-bonding power, has the largest K_{SV} value. Thus, the hydrogens of the alcohols' hydroxy groups participate in the interactions.

3.3. Results of Calculations. The excitation energies and oscillator strengths of singlet−singlet electronic transitions were calculated for the molecules TACV−Py′ and TACV−Ph′ (Chart 1), which are models of the molecules studied experimentally. These models contain a methyl group instead of a hydroxyethoxymethyl substituent at the N(3) position of the tricyclic system. The results of calculations at the PBE0/6-311+G(2df,2pd) level of theory are presented in Table 4. For TACV−Ph′ in the gas phase, the results of the present calculations are qualitatively similar to those of previous calculations performed at the B3LYP/6-31G(d) level.[13] However, inclusion of the bulk solvent effect into the computation provides more reliable results. As shown in Tables 1 and 4 and Figure 1, the calculated energy of the $S_0 \rightarrow S_1$ transition for TACV−Ph′ in CH_3OH corresponds almost exactly to the experimental λ_{max}^A of the long-wavelength absorption band in the same solvent (λ_{max}^A = 32 360 cm^{-1}), and the experimental absorption maximum of TACV−Py is shifted by 1460 cm^{-1} to higher frequencies as compared to the computed energy of the $S_0 \rightarrow S_1$ transition for TACV−Py′. For both compounds, the first excited singlet state has $\pi \rightarrow \pi^*$ character, and it lies about 11 000 cm^{-1} below the lowest energy $n \rightarrow \pi^*$ transition (TACV−Py′, $S_0 \rightarrow S_5$; TACV−Ph′, $S_0 \rightarrow S_7$).

TABLE 4: Calculated (PBE0/6-311+G(2df,2pd)) Excitation Energies ($S_0 \rightarrow S_i$, in 10^3 cm^{-1}) and Oscillator Strengths (in Parentheses) of Vertical Transition for TACV−Ph′ and TACV−Py′ in a Vacuum[a] and CH_3OH Solution (Including the Bulk Solvent Effect)

	TACV−Ph′		TACV−Py′	
	in a vacuum	in CH_3OH	in a vacuum	in CH_3OH
S_1	29.92 (0.098)	32.02 (0.225)	27.64 (0.072)	29.21 (0.137)
S_2	34.55 (0.010)	36.98 (0.100)	35.00 (0.000)	36.01 (0.389)
S_3	37.49 (0.452)	38.01 (0.483)	36.18 (0.056)	37.32 (0.004)
S_4	38.70 (0.005)	39.14 (0.357)	36.55 (0.480)	37.57 (0.392)
S_5	39.61 (0.489)	40.48 (0.378)	38.92 (0.000)*	39.20 (0.200)
S_6	40.43 (0.021)	41.80 (0.008)	39.29 (0.005)	40.49 (0.287)
S_7	40.56 (0.016)*	42.24 (0.015)	40.00 (0.382)	41.53 (0.069)

[a] The $n \rightarrow \pi^*$ transitions are labeled with an asterisk; the other transitions are of the $\pi \rightarrow \pi^*$ type.

TABLE 5: Calculated Excitation Energy ($S_0 \rightarrow S_1$, in 10^3 cm^{-1}) and Oscillator Strength (in Parentheses) of the Lowest Energy Transition for the Hydrogen-Bonded Complex of TACV−Ph′ and TACV−Py′ with a CH_3OH Molecule in a Vacuum and CH_3OH Solution

complex	in a vacuum	in CH_3OH
	TACV−Ph′	
N(1)···CH_3OH	30.86 (0.118)	32.11 (0.249)
C═O···CH_3OH	30.81 (0.124)	32.09 (0.251)
N(4)···CH_3OH	30.95 (0.111)	32.52 (0.237)
	TACV−Py′	
N(1)···CH_3OH	28.70 (0.082)	29.49 (0.147)
C═O···CH_3OH	28.56 (0.088)	29.49 (0.157)
N(4)···CH_3OH	28.77 (0.076)	29.92 (0.142)
N(13)···CH_3OH	26.43 (0.070)	28.55 (0.134)

To determine the specific (microscopic) solvent effect on the transition energies and intensities, the calculations were performed for the complexes of a single CH_3OH molecule hydrogen bonded with the solute molecule at the position N-1, N-4, C═O, or N-13. The complexes were considered to be either isolated in a vacuum or embedded in a dielectric continuum mimicking the bulk properties of the solvent. The results of calculations at the PBE0/6-311+G(2df,2pd) level are shown in Table 5. Formation of the hydrogen-bonded complexes at the N(1), C═O, and N(4) sites increases the $S_0 \rightarrow S_1$ excitation energy by about 1000 cm^{-1} in a vacuum and by 100−700 cm^{-1} in CH_3OH solution. In contrast, the $S_0 \rightarrow S_1$ excitation energy for the TACV−Py′···CH_3OH complex at the N(13) site is predicted to be 1210 and 660 cm^{-1} lower than that for the free TACV−Py′ molecule in a vacuum and CH_3OH solution, respectively.

The calculated relative energies of TACV−Py′ and TACV−Ph′ complexed at various sites with CH_3OH in their ground S_0

TABLE 6: Relative Energies[a] (in kcal/mol) of TACV−Ph′ and TACV−Py′ Complexed with the CH_3OH Molecule in a Vacuum and CH_3OH Solution Calculated for the Ground (S_0) and First Excited (S_1) States

complex	in a vacuum	in CH_3OH
	TACV−Ph′	
N(1)···CH_3OH	−6.8/−4.1	−0.9/−0.6
C═O···CH_3OH	−7.7/−5.2	−2.0/−1.8
N(4)···CH_3OH	−10.5/−7.6	+0.4/+1.8
	TACV−Py′	
N(1)···CH_3OH	−6.4/−3.4	−1.3/−0.5
C═O···CH_3OH	−7.5/−4.9	−2.0/−1.2
N(4)···CH_3OH	−10.7/−7.5	+0.6/+2.6
N(13)···CH_3OH	−6.5/−10.0	−2.8/−4.7

[a] The difference of the electronic total energies of the complex and free molecules in their S_0/S_1 states.

and excited S_1 states are presented in Table 6. It is evident that the solvation effect plays a crucial role in stabilizing the complex. The complex with CH_3OH attached at the N(4) atom of either TACV−Py′ or TACV−Ph′ is calculated to be the most stable in a vacuum. In contrast, when the bulk solvent effect is taken into account, this complex-formation reaction becomes slightly endoergic. In the ground S_0 state of the complexes solvated in methanol, these are interactions of the C═O group of TACV−Ph′ and the N(13) atom of TACV−Py′ with CH_3-OH, which lead to the most stable complexes. All but one of the hydrogen-bonded complexes are destabilized by excitation to the S_1 state regardless of the environment. The complex of TACV−Py′ with CH_3OH attached at the N(13) atom of the pyridine moiety is predicted to be stabilized by excitation to the S_1 state by 3.5 and 1.9 kcal/mol in a vacuum and CH_3OH solution, respectively.

Changes in the relative energies of the complexes upon excitation are consistent with the charge-transfer character of the S_1 state. The TDDFT calculations revealed that in the TACV−Py′ and TACV−Ph′ molecules, the S_1 state wave functions are dominated by the HOMO → LUMO transition. The shapes of the molecular orbitals involved in this transition for the TACV−Py′ molecule are shown in Figure 7. The corresponding molecular orbitals for TACV−Ph′ are similar. Note that the HOMO and LUMO are localized on different parts of the TACV−Py′ molecule; the HOMO is on the tricyclic imidazopurine moiety and the LUMO is on the pyridine ring. Therefore, the $S_0 \rightarrow S_1$ excitation involves substantial transfer of the electronic charge from the tricyclic imidazopurine system to the pyridyl or phenyl substituent. As a result, the N(13) atom of the TACV−Py′ molecule becomes more negative in the excited S_1 state, thus increasing its hydrogen-bond-acceptor ability.

4. Conclusion

Both experimental results and quantum-chemical calculations are consistent and provide an explanation of the different fluorescence properties of 9-oxo-imidazo[1,2-*a*]purine derivatives bearing pyridyl or phenyl substituents at the C(6) position. The S_1 state of the molecules TACV−Py and TACV−Ph as well as those containing pyridylphenyl and biphenylyl substituents, TACV−Ph−Py and TACV−Ph−Ph, has a charge-transfer character. The dipole-moment changes associated with the excitation of the molecules are large ($\Delta\mu$ = 11.6 D for TACV−Py and $\Delta\mu$ = 7.3 D for TACV−Ph from experiment; and $\Delta\mu$ = 15.2 D for TACV−Py′ and $\Delta\mu$ = 10.0 D for TACV−Ph′ from calculations). Upon excitation the electronic charge is transferred from a tricyclic imidazo[1,2-*a*]purine system to a substituent at the C(6) position. Therefore, in the excited S_1 state of TACV−Py and TACV−Ph−Py, the negative charge on the pyridine nitrogen atom increases, enhancing its ability to participate as an H acceptor in the hydrogen bond. The intermolecular interaction between the hydroxyl group of the alcohol and the nitrogen atom of the pyridine moiety in the excited S_1 state of TACV−Py and TACV−Ph−Py leads to an efficient quenching of fluorescence. Although all of the molecules studied have other sites in the tricyclic 9-oxo-imidazo-[1,2-*a*]purine system that could act as hydrogen-bond acceptors, their interactions with the alcohol molecules in the excited S_1 state are diminished due to the overall reduced electronic charge on the heterocycles' tricyclic moiety. Among the compounds studied in this work, the biphenylyl derivative TACV−Ph−Ph appears to be the most suitable for biological and medical applications because it exhibits a strong absorption in the long-wavelength region (λ > 300 nm), an intense fluorescence regardless of the medium, and a moderately long lifetime. On the other hand, molecules have been used as molecular probes that exhibit fluorescence behavior similar to those of the compounds containing pyridyl and pyridylphenyl substituents.[43−46] Therefore, TACV−Py, TACV−Ph−Py, and other molecules based on these novel fluorophores may find applications as sensors of the hydroxyl groups in microenvironments.

Acknowledgment. Calculations were performed at the Poznan Supercomputer Center (PCSS).

References and Notes

(1) Boryski, J.; Golankiewicz, B.; De Clercq, E. *J. Med. Chem.* **1988**, *31*, 1351.
(2) Dosjanjh, M. K.; Chenna, A.; Kim, E.; Fraenkel-Conrat, H.; Samson, L.; Singer, B. *Proc. Natl. Acad. Sci. U.S.A.* **1994**, *91*, 1024.
(3) RajBhandary, U. L.; Chang, S. H.; Stuart, A.; Faulkner, R. D.; Hoskinson, R. M.; Khorana, H. G. *Proc. Natl. Acad. Sci. U.S.A.* **1967**, *57*, 751.
(4) Sattsangi, P. D.; Leonard, N. J.; Frihart, C. R. *J. Org. Chem.* **1977**, *42*, 3292.
(5) Golankiewicz, B.; Ostrowski, T.; Andrei, G.; Snoeck, R.; DeClercq, E. *J. Med. Chem.* **1994**, *37*, 3187.
(6) Balzarini, J.; Ostrowski, T.; Goslinski, T.; De Clercq, E.; Golankiewicz, B. *Gene Ther.* **2002**, *9*, 1173.
(7) Loregien, A.; Gatti, R.; Palu, G.; De Palo, E. F. *J. Chromatogr., B* **2001**, *764*, 289.
(8) Czaplicki, J.; Bohner, T.; Habermann, A.-K.; Folkers, G.; Milton, A. *J. Biomol. NMR* **1996**, *8*, 261.
(9) Goslinski, T.; Golankiewicz, B.; De Clercq, E.; Balzarini, J. *J. Med. Chem.* **2002**, *45*, 5052.
(10) Goslinski, T.; Januszczyk, P.; Wenska, G.; Golankiewicz, B.; DeClerq, E.; Balzarini, J. *Nucleosides Nucleotides* **2005**, *24*, 571.
(11) Goslinski, T.; Wenska, G.; Golankiewicz, B.; Balzarini, J.; DeClercq, E. *Nucleosides Nucleotides* **2003**, *22*, 911.
(12) Ostrowski, T.; Zeidler, J.; Goslinski, T.; Golankiewicz, B. *Nucleosides Nucleotides* **2000**, *19*, 1911.
(13) Wenska, G.; Koput, J.; Insinska-Rak, M.; Golankiewicz, B.; Goslinski, T.; Ostrowski, T. *J. Photochem. Photobiol., A* **2004**, *163*, 171.
(14) Eaton, D. F. *Pure Appl. Chem.* **1998**, *60*, 1107.
(15) Milewski, M.; Baksalary, J.; Antkowiak, P.; Augustyniak, W.; Binkowski, M.; Karolczak, J.; Komar, D.; Maciejewski, A.; Szymanski, M.; Urjasz, W. *J. Fluoresc.* **2000**, *10*, 89.
(16) Karolczak, J.; Komar, D.; Kubicki, J.; Szymanski, M.; Wróżowa, T.; Maciejewski, A. *Bull. Pol. Acad. Sci., Chem.* **1999**, *47*, 361.
(17) Karolczak, J.; Komar, D.; Kubicki, J.; Wrozowa, T.; Dobek, K.; Ciesielska, B.; Maciejewski, A. *Chem. Phys. Lett.* **2001**, *344*, 154.
(18) Wróżowa, T.; Ciesielska, B.; Komar, D.; Karolczak, J.; Maciejewski, A.; Kubicki, J. *Rev. Sci. Instrum.* **2004**, *75*, 3107.
(19) Adamo, C.; Barone, V. *J. Chem. Phys.* **1999**, *110*, 6158.
(20) Krishnan, R.; Binkley, J. S.; Seeger, R.; Pople, J. A. *J. Chem. Phys.* **1980**, *72*, 650.
(21) Barone, V.; Cossi, M. *J. Phys. Chem. A* **1998**, *102*, 1995.
(22) Frisch, M. J.; Trucks, G. W.; Schlegel, H. B.; Scuseria, G. E.; Robb, M. A.; Cheeseman, J. R.; Montgomery, J. A., Jr.; Vreven, T.; Kudin, K. N.; Burant, J. C.; Millam, J. M.; Iyengar, S. S.; Tomasi, J.; Barone, V.; Mennucci, B.; Cossi, M.; Scalmani, G.; Rega, N.; Petersson, G. A.;

Nakatsuji, H.; Hada, M.; Ehara, M.; Toyota, K.; Fukuda, R.; Hasegawa, J.; Ishida, M.; Nakajima, T.; Honda, Y.; Kitao, O.; Nakai, H.; Klene, M.; Li, X.; Knox, J. E.; Hratchian, H. P.; Cross, J. B.; Adamo, C.; Jaramillo, J.; Gomperts, R.; Stratmann, R. E.; Yazyev, O.; Austin, A. J.; Cammi, R.; Pomelli, C.; Ochterski, J. W.; Ayala, P. Y.; Morokuma, K.; Voth, G. A.; Salvador, P.; Dannenberg, J. J.; Zakrzewski, V. G.; Dapprich, S.; Daniels, A. D.; Strain, M. C.; Farkas, O.; Malick, D. K.; Rabuck, A. D.; Raghavachari, K.; Foresman, J. B.; Ortiz, J. V.; Cui, Q.; Baboul, A. G.; Clifford, S.; Cioslowski, J.; Stefanov, B. B.; Liu, G.; Liashenko, A.; Piskorz, P.; Komaromi, I.; Martin, R. L.; Fox, D. J.; Keith, T.; Al-Laham, M. A.; Peng, C. Y.; Nanayakkara, A.; Challacombe, M.; Gill, P. M. V.; Johnson, B.; Chen, W.; Wong, M. W.; Gonzales, C.; Pople, J. A. *Gaussian 03*, revision C.02; Gaussian, Inc.: Pittsburgh, PA, 2003.

(23) Lakowicz, J. R. *Principles of Fluorescence Spectroscopy*; Kluwer Academic/Plenum Publishers: New York, 1999.

(24) Lippert, E. *Z. Electrochem.* **1957**, *61*, 962.

(25) Mataga, N.; Kaifu, Y.; Koizumi, M. *Bull. Chem. Soc. Jpn.* **1956**, *29*, 465.

(26) Reichardt, C. *Solvents and Solvent Effects in Organic Chemistry*; VSH: Weinheim, 1988.

(27) Kamlet, M. J.; Abboud, J. L. M.; Abraham, M. H.; Taft, R. W. *J. Org. Chem.* **1983**, *48*, 2877.

(28) Flom, S. R.; Barbara, P. F. *J. Phys. Chem.* **1985**, *89*, 4489.

(29) Inoue, H.; Hida, M.; Nakashima, N.; Yoshihara, K. *J. Phys. Chem.* **1982**, *86*, 3184.

(30) Jones, G., II; Feng, Z.; Bergmark, W. R. *J. Phys. Chem.* **1994**, *98*, 4511.

(31) Moog, R. S.; Burozski, N. A.; Desai, M. M.; Good, W. R.; Silvers, C. D.; Thompson, P. A.; Simon, J. D. *J. Phys. Chem.* **1991**, *95*, 8466.

(32) Yatsuhashi, T.; Nakjima, Y.; Shimada, T.; Inoue, H. *J. Phys. Chem. A* **1998**, *102*, 3018.

(33) Nayak, M. K.; Dogra, S. K. *J. Photochem. Photobiol., A* **2005**, *169*, 299.

(34) Hallidy, L. A.; Topp, M. R. *J. Phys. Chem.* **1978**, *82*, 2415.

(35) Saroja, G.; Ramachandram, B.; Saha, S.; Samanta, A. *J. Phys. Chem. B* **1999**, *103*, 2906.

(36) Herbich, J.; Hung, C.-Y.; Thummel, R. P.; Waluk, J. *J. Am. Chem. Soc.* **1996**, *118*, 3508.

(37) Herbich, J.; Rettig, W.; Thummel, R. P.; Waluk, J. *Chem. Phys. Lett.* **1992**, *195*, 556.

(38) Waluk, J. *Acc. Chem. Res.* **2003**, *36*, 832.

(39) Harju, T. O.; Huizer, A. H.; Varma, C. A. G. O. *Chem. Phys.* **1995**, *200*, 215.

(40) Yatsuhashi, T.; Nakajima, Y.; Shimada, T.; Inoue, H. *J. Phys. Chem. A* **1998**, *102*, 3018.

(41) Marimoto, A.; Yatsuhashi, T.; Shimada, T.; Biczok, L.; Tryk, D. A.; Inoue, H. *J. Phys. Chem. A* **2001**, *105*, 10488.

(42) Avouris, P.; El-Sayed, M. A.; Gelbart, W. M. *Chem. Rev.* **1977**, *77*, 793.

(43) Langhals, H. *Anal. Lett.* **1991**, *23*, 2243.

(44) Saroja, G.; Samanta, A. *Chem. Phys. Lett.* **1995**, *246*, 506.

(45) Wintgens, V.; Amiel, C. *J. Photochem. Photobiol., A* **2004**, *168*, 217.

(46) Rettig, W., Strehmel, B., Schrader, S., Seifert, H., Eds. *Applied Fluorescence in Chemistry, Biology and Medicine*; Springer: Berlin, Heidelberg, 1999.